Molecular Therapy
Oncolytics
Original Article

Enhanced Safety and Efficacy of Oncolytic VSV Therapy by Combination with T Cell Receptor Transgenic T Cells as Carriers

Michael Karl Melzer,[1] Lisa Zeitlinger,[1] Sabine Mall,[2,3] Katja Steiger,[4] Roland M. Schmid,[1] Oliver Ebert,[1] Angela Krackhardt,[2,3] and Jennifer Altomonte[1]

[1]Klinik und Poliklinik für Innere Medizin II, Klinikum rechts der Isar, Technical University, 81675 Munich, Germany; [2]Klinik und Poliklinik für Innere Medizin III, Klinikum rechts der Isar, Technical University, 81675 Munich, Germany; [3]German Cancer Consortium of Translational Cancer Research (DKTK) and German Cancer Research Center (DKFZ), 69120 Heidelberg, Germany; [4]Institut für Pathologie, Klinikum rechts der Isar, Technical University, 81675 Munich, Germany

Vesicular stomatitis virus (VSV) represents an attractive oncolytic virotherapy platform because of its potent tumor cell-killing and immune-stimulating properties; yet the clinical translation of VSV faces numerous challenges, such as inefficient systemic delivery and severe side effects such as neurotoxicity. We hypothesized that we could overcome these limitations and simultaneously enhance the therapy, by combining VSV with adoptively transferred T cell receptor (TCR) transgenic T cells as carrier cells. We show that $CD8^+$ T central memory cells ($CD8^+$ T cm) can be efficiently loaded with VSV, they support intracellular virus production, and they can efficiently transfer VSV to tumor cells without compromising their own viability or antitumor reactivity. Loading VSV onto $CD8^+$ T cm not only improves the safety compared with systemic administration of naked virus, but this approach also allows for an effective delivery of virus to its tumor target, resulting in an effective combination therapy in NSG mice bearing subcutaneous human acute myeloid leukemia (AML) tumors. We conclude that the combination of potent tumor debulking provided by the oncolytic VSV with the added effector functions afforded by the cytotoxic immune carrier cells results in a potent and safer immunotherapeutic, which can be further developed for clinical translation.

INTRODUCTION

Acute myeloid leukemia (AML) is the most common type of blood cancer[1,2] and is characterized by a poor prognosis.[3] Although new therapeutic approaches are being investigated,[3,4] the standard of care still includes chemotherapy schemes and hematopoietic stem cell transplantation.[3] Elderly patients are often not eligible for intensive therapies due to diminished health status, which contributes to a poor prognosis.[3,5,6] There is therefore a crucial need for the development of improved therapeutic approaches.

Oncolytic viruses have emerged as promising cancer therapeutics because of their tumor-selective replication and cytolysis, and their potential to induce systemic antitumor immune responses.[7] Despite encouraging progress in clinical application, systemic delivery of oncolytic viruses remains a major challenge because of inactivation by blood components, nonspecific uptake, and clearance by the reticuloendothelial system,[8–11] which restrict the amount of virus that can reach the tumor after injection into the bloodstream. Furthermore, the extravasation of viral particles from the feeding blood vessels into the tumor is limited.[12] The use of carrier cells has emerged as an elegant strategy for shielding oncolytic viruses and delivering them specifically to the tumor site following systemic administration.[13,14] This is a particularly attractive approach for targeting tumors that are not easily accessible for direct intratumoral injection or for treatment of metastatic disease. Furthermore, if the carrier cells themselves provide a cytotoxic effector function, the combination can result in synergistic and multimechanistic responses. Adoptively transferred transgenic T cells have been shown to chaperone oncolytic vesicular stomatitis virus (VSV) to target tumor sites and mediate potent antitumor effects in immune-competent mouse models.[15–17] Furthermore, it was demonstrated that the VSV mutant, recombinant VSV (rVSV)-ΔM51, could be loaded onto tumor-reactive T cells and be successfully shuttled to the tumor, thereby mediating enhanced responses compared with monotherapies.[18–20]

VSV is an attractive oncolytic virus due to its ability to efficiently kill a broad range of tumor cells and to express transgenes to high levels, in a variety of model systems.[16,17,21–25] Although the clinical translation of wild-type VSV has been hindered because of its neurovirulence,[26,27] various engineering strategies have been explored to improve safety,[28] and rVSV vectors expressing interferon beta (IFN-β) have already entered phase I clinical trials (ClinicalTrials.gov: NCT03017820, NCT031624, and NCT01628640). In the proof-of-principle study presented here, we have utilized rVSV vectors based on the wild-type VSV genome; however, we expect our findings to

Received 16 November 2018; accepted 5 December 2018;
https://doi.org/10.1016/j.omto.2018.12.001.

Correspondence: Jennifer Altomonte, Klinik und Poliklinik für Innere Medizin II, Klinikum rechts der Isar, Technical University, Ismaningerstrasse 22, 81675 Munich, Germany.
E-mail: jennifer.altomonte@tum.de

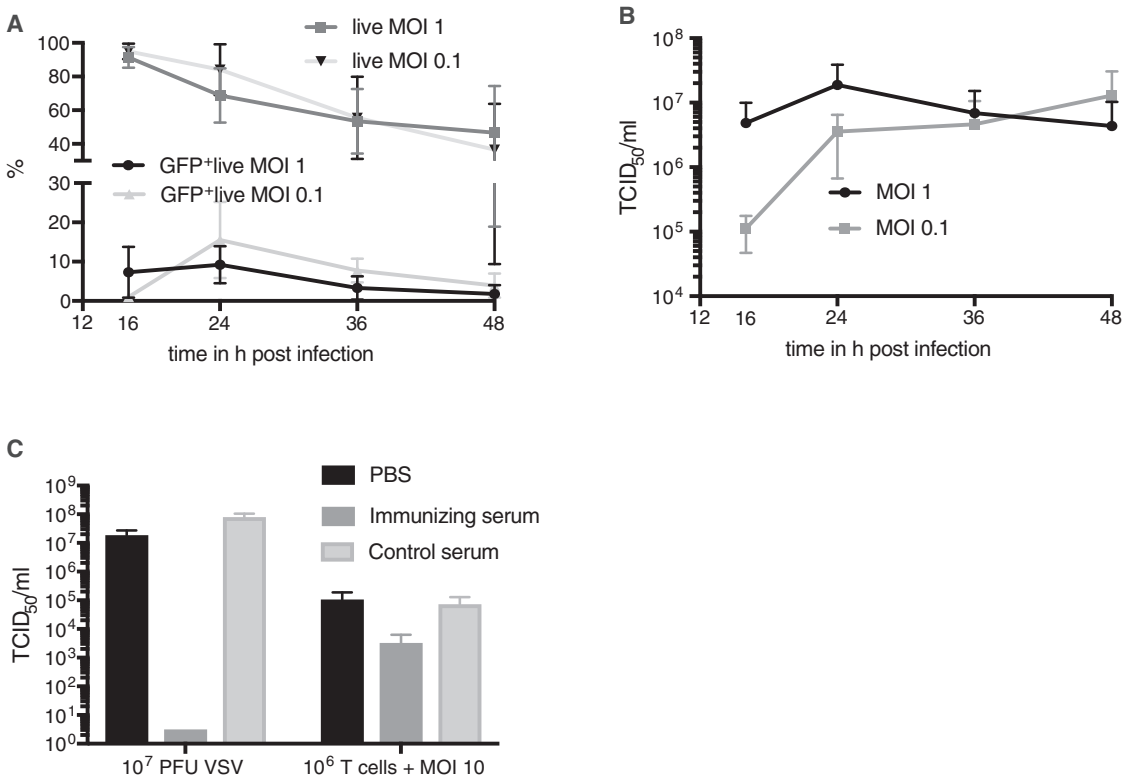

Figure 1. Characterization of VSV Infection in Human Pan T Cells

(A) Pan T cells isolated from human blood were infected with rVSV vectors expressing GFP at an MOI of 1 or 0.1 and monitored for 16, 24, 36, and 48 hr. The washed cell populations were analyzed by flow cytometry for GFP expression as well as viability by measuring 7-AAD uptake. Means ± SD for the percentages of whole living cells, as well as GFP^+ living cells, are shown for four different T cell donors for MOI 1 and for two different T cell donors for MOI 0.1. (B) $TCID_{50}$ analysis of culture supernatants from T cells infected at an MOI of 1 or 0.1, using cells isolated from four or two donors, respectively. Means ± SD are shown on a logarithmic scale. (C) Shielding of VSV from neutralizing antibodies was examined. $TCID_{50}$ assay was performed for naked VSV after incubation with neutralizing antibodies, as well as for VSV that was shielded by T cells. Means ± SD are shown.

be applicable to other, potentially safer, VSV-based vectors, which could result in even further enhanced responses because of their improved safety profiles and the ability to administer higher doses.

Human T cell receptor transgenic T cells (TCR T cells) specific for a peptide of myeloperoxidase (MPO_5), presented on the HLA-B*07:02, function as efficient anti-leukemia agents.[29] Furthermore, those T cells can be tracked by positron emission tomography (PET) imaging,[30,31] which offers an attractive option to effectively monitor T cells *in vivo*. Here, we use this well-characterized model system to investigate the combination of human TCR T cells together with VSV in an *in vivo* setting. Screening experiments revealed that T cells not only can be loaded with VSV and support subsequent virus amplification, but they can also efficiently shield VSV from neutralizing antibodies. Due to evidence that the central memory compartment of the $CD8^+$ T cell ($CD8^+$ T cm) population is an effective adoptive T cell therapy,[32] we chose to focus on this T cell subpopulation for our combination approach. We demonstrate that VSV can be loaded on $CD8^+$ T cm, resulting in only minimal impairment of cell viability and providing a more potent antitumor efficacy compared with a VSV-monotherapy in co-culture with the targeted ML2 leukemia cells *in vitro*. Studies in immune-deficient NOD Cg-Prkdc^{scid} Il2rg^{tm1Wjl}/SzJ (NSG) mice revealed that the T cell-associated VSV has a better safety profile after systemic application than non-cell-bound ("naked") VSV. Furthermore, this combination also led to a more rapid and efficient tumor cell killing than virus therapy alone. Based on these data, we conclude that the combination of oncolytic virus therapy with human tumor-specific immune effector cells as virus carriers could provide a significant therapeutic benefit over either monotherapy and should be further developed for clinical translation.

RESULTS

VSV Is Able to Infect and Replicate in T Cells while Being Protected from Neutralization

In order to screen VSV for its ability to infect and replicate in T cells, we isolated PBMCs from human blood and infected them with rVSV vectors expressing GFP, which is based on the unmodified VSV backbone, at an MOI of 0.1 and 1. Viral-mediated GFP expression was measured by fluorescence-activated cell sorting (FACS) analysis at various time points post-infection (Figure 1A). GFP expression was

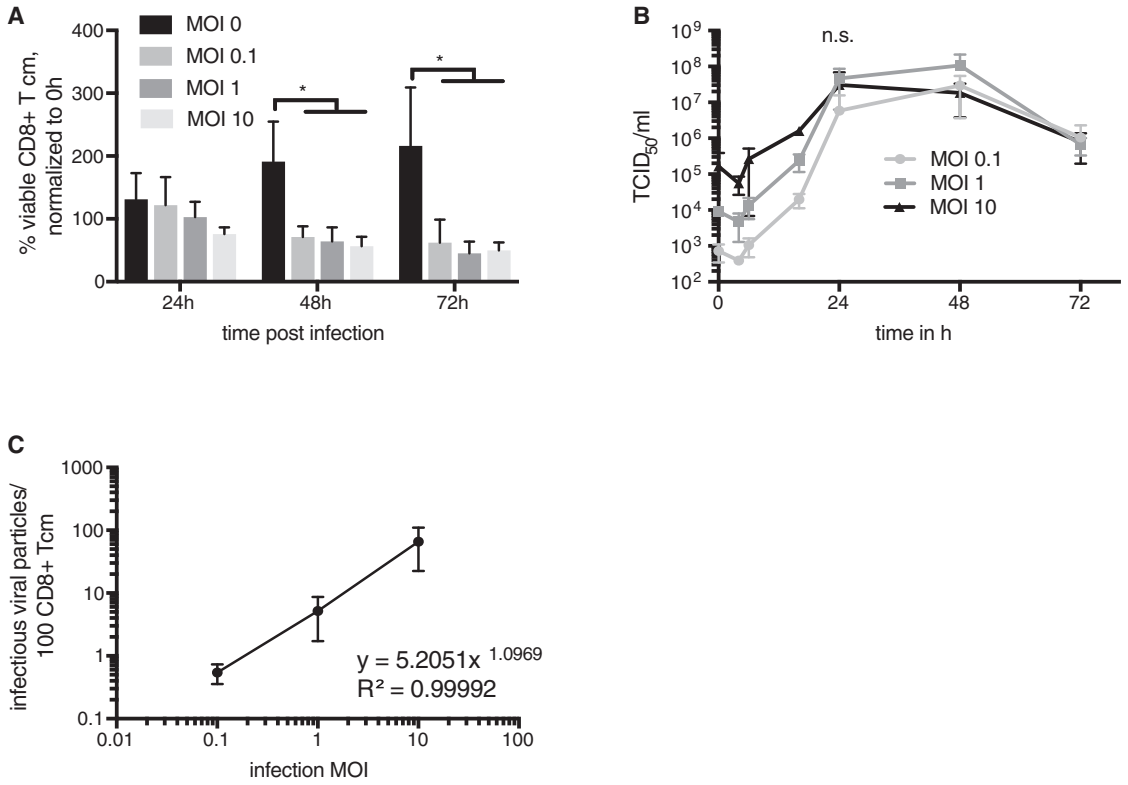

Figure 2. CD8$^+$ T cm Can Be Infected with VSV and Transfer Virions to Susceptible Cells

CD8$^+$ T cm were infected with indicated MOIs of rVSV vectors expressing GFP and cultured until the indicated time points. (A) CD8$^+$ T cm were counted. Percentage of viable cells normalized to time point 0 hr are shown. Means ± SD of three independent experiments, performed in triplicates from three different CD8$^+$ T cm donors, are shown. Statistical analysis was performed by two-way ANOVA with Bonferroni post-test (*$p < 0.05$). (B) $TCID_{50}$ assays were performed from tissue culture supernatants at the indicated time points. The experiment was performed three times in triplicates from different donors, and the means ± SD are shown. Two-way ANOVA with Bonferroni post-test showed no significant difference between the different MOIs at 24 hr after infection. (C) Infected CD8$^+$ T cm were co-cultured with BHK-21 cells. The percentage of GFP$^+$ BHK-21 cells was used to calculate the viral load on the CD8$^+$ T cm surface that could be transferred to other cells. The experiment was performed in triplicates using CD8$^+$ T cm derived from three individual donors. Means ± SD are shown. The best-fitting equation is given.

detected as early as 16 hr after infection, with the level increasing to 9.3% at 24 hr for MOI 1 and 15.51% for MOI 0.1. These results indicate that pan T cells can be infected, at least to an extent, and allow for VSV-mediated transgene expression. Interestingly, GFP expression decreased again at later time points. Analysis of T cell viability by 7-aminoactinomycin D (7-AAD) staining revealed that the decrease in GFP expression corresponds with a reduction of T cell viability after 24 hr of infection (Figure 1A). Despite this gradual loss of viability, pan T cells were rather resistant to VSV infection compared with tumor cells, with almost 50% of the T cell population remaining viable after a 48-hr infection. Nevertheless, a peak in replication kinetics was observed at 24 hr after infection, with titers reaching more than 10^7 $TCID_{50}$/mL after infection at an MOI of 1 (Figure 1B). The titers for T cells that had been infected with MOI 0.1 consistently increased until 48 hr after infection and also reached a level of approximately 10^7 $TCID_{50}$/mL. In a last screening experiment, we investigated whether VSV loaded onto T cells could be protected from antibody-mediated neutralization (Figure 1C). Even though naked virus was extremely susceptible to inactivation by neutralizing serum, T cells that were loaded with an equivalent amount of virus were able to effectively shield VSV and protect it from neutralizing antibodies. Taken together, we can conclude that, although T cells are rather resistant to VSV-mediated cytotoxicity, and only a small proportion of cells become actively infected, they can internalize VSV, protecting it from inactivation, and produce and release high titers of virus progeny. These data would argue that T cells are excellent candidates as carrier cells for systemic delivery of oncolytic VSV, while potentially providing an additional therapeutic component via their cytotoxic effector functions.

CD8$^+$ T cm Can Internalize and Produce VSV and Carry VSV on Their Cell Surface

Knowing that human CD8$^+$ T cm have been described previously to have superior antitumor effector functions than other T cell subpopulations,[32,33] we chose to focus on CD8$^+$ T cm in the remainder of our investigations. To determine the sensitivity of CD8$^+$ T cm to VSV infection, we measured cell viability by trypan blue assay at various time points post-infection (Figure 2A). No significant difference

could be observed between uninfected and infected $CD8^+$ T cm after 24 hr, regardless of the amount of input virus, indicating a relative resistance to VSV-mediated killing, although there was a significant decrease of cell viability at later time points (48 and 72 hr) after infection. Nevertheless, viral titers increased rapidly in a dose-dependent manner at early time points after infection, reaching their peaks at approximately equal levels at 24 hr post-infection, demonstrating that a productive infection had taken place (Figure 2B). Because it has been previously reported that T cells can carry VSV on their cell surface,[18] we designed an experiment to determine whether, and to which extent, this was the case in our hands. $CD8^+$ T cm were infected with various MOIs of rVSV vectors expressing GFP and then co-cultured with BHK-21 cells, which are highly susceptible to VSV infection. After a 6-hr co-culture, the culture supernatant containing the T cells was washed away, and the percentage of GFP^+ BHK-21 cells was determined by FACS analysis, as a surrogate marker to calculate the percentage of virus initially associated with the T cell surface that could be directly transferred to other cells, because internalized virus would not have had time to replicate during the short infection time prior to the co-culture. We calculated a non-linear correlation between the input MOI and the percentage of directly transferrable, infectious, T cell-bound virus, which resulted in the following equation: $y = 5.2051x^{1.0969}$ ($R^2 = 0.99992$) (Figure 2C). For y, we take the percentage of infected T cells, and for x, we take the input MOI. From these data, we conclude that $CD8^+$ T cm can carry VSV, both on the surface and intracellularly.

ML2 Leukemia Cells Are Efficiently Killed by VSV and TCR T Cells

The susceptibility of ML2B7-FLuc leukemia cells to infection with increasing MOIs of rVSV was measured by luciferase assay to determine changes in cell viability over time. Because these cells also stably express GFP, providing a fast and easy fluorescence microscopy and FACS method for distinguishing the tumor cells from the T cells in co-culture, we chose to use an rVSV vector expressing the herpes simplex virus I thymidine kinase reporter (rVSV-tk) for this experiment, instead of rVSV vectors expressing GFP, to avoid interference of the viral GFP with the tumor cell-expressed GFP. A fast and dose-responsive reduction in luciferase reporter expression indicates that ML2B7-Fluc cells are highly sensitive to the cytopathic effects of VSV, with the exception of the lowest MOI tested (0.001), which resulted in delayed virus-mediated cell killing (Figure 3A). Viral replication was confirmed by virus growth curves as determined by $TCID_{50}$ assays from culture supernatants at indicated time points (Figure 3B). High titers (up to 10^7–10^8 $TCID_{50}$/mL) could be observed as early as 16-hr post-infection in a dose-responsive manner at early time points after infection. Cell viability of ML2B7-Fluc cells when treated with TCR T cells and control T cells, either alone or loaded with VSV-tk, was determined by luciferase assay (Figure 3C). A significant advantage of a combination therapy consisting of TCR T cells and VSV, compared with the combination of unspecific T cells and VSV, was evident. A trend of enhanced cytotoxicity was observed when comparing TCR T cells loaded with VSV and TCR T cells alone. TCR T cell monotherapy was not more efficient than the combination of control T cells with VSV. Taking into consideration that 10^5 tumor cells were treated in that 1:20 ratio, meaning only 5,000 T cells were applied, we can appreciate the degree to which the cytotoxic effect is mediated by VSV. The T cells had been infected at an MOI of 0.1, which results in only 0.42% T cells that can directly transfer VSV, according to the equation from Figure 2. The calculation of the absolute amount of directly transferable virus indicates that only 21 plaque-forming units (PFU) were applied in the combination approach. This translates to less than the lowest amount of naked VSV (100 PFU) that was added to the ML2B7-Fluc cells at MOI 0.001 in Figure 3A. Nevertheless, if we compare the means of cell viability in Figures 3A and 3C at 24 hr, it seems that the effect of VSV is substantially greater when applied together with T cells. This observation indicates that T cells, regardless of their transduction status, can amplify the amount of internalized input virus, and that TCR-transduced T cells can further enhance the therapy through their contribution of cytotoxic effector functions. However, it has to be considered that a direct comparison here is not easy to make. Due to the fact that the T cells would produce virus, as well as directly transfer it from their cell surface, the amounts of virus effectively applied in each case is not equal, thereby limiting our ability to correctly interpret such a comparison. In contrast, the comparison between control T cells and TCR T cells, when they are both loaded with VSV, clearly demonstrates that TCR T cells enhance the oncolytic potential of VSV. Here, both T cell groups contain the same amount of VSV, allowing us to directly compare the two conditions. $TCID_{50}$ analysis of co-culture supernatants showed significantly lower titers in the treatment group with specific TCR T cells compared with the group with control T cells (Figure 3D). Importantly, IFN-γ concentrations in the co-culture supernatants indicate a specific TCR T cell activation, and pre-infection with rVSV-tk neither interferes nor causes a nonspecific activation (Figure 3E). These results indicate that a combination of TCR T cells with oncolytic VSV could provide beneficial therapeutic effects compared with VSV monotherapy at a comparable dose, and potentially also compared with TCR T cells as a monotherapy.

VSV Toxicity in NSG Mice Is Reduced by $CD8^+$ T cm-Mediated Delivery

Before investigating efficacy *in vivo*, we sought to determine the maximum tolerated doses (MTDs) of naked VSV versus VSV delivered via $CD8^+$ T cm. Increasing doses of naked rVSV vectors expressing GFP or 10^7 $CD8^+$ T cm pre-infected at increasing MOIs of rVSV vectors expressing GFP were injected by tail vein in nontumor-bearing NSG mice. Mice were monitored for 3 weeks for toxic events and euthanized at humane endpoints. Systemic injection of naked virus resulted in toxicity at substantially lower doses compared with T cm-mediated VSV delivery (Figure 4A; Table 1). Analysis of brains by $TCID_{50}$ revealed that replication-competent VSV could be detected in the brains, as well as other organs, at the time of euthanasia, predominantly in mice that had received naked VSV (Figure 4B; Figure S1). The injected dose of cell-associated virus was calculated according to the equation derived from Figure 2C, and the results are shown in the table summarizing the toxicity data (Table 1). Because even the lowest tested dose of naked virus resulted in toxicity, for

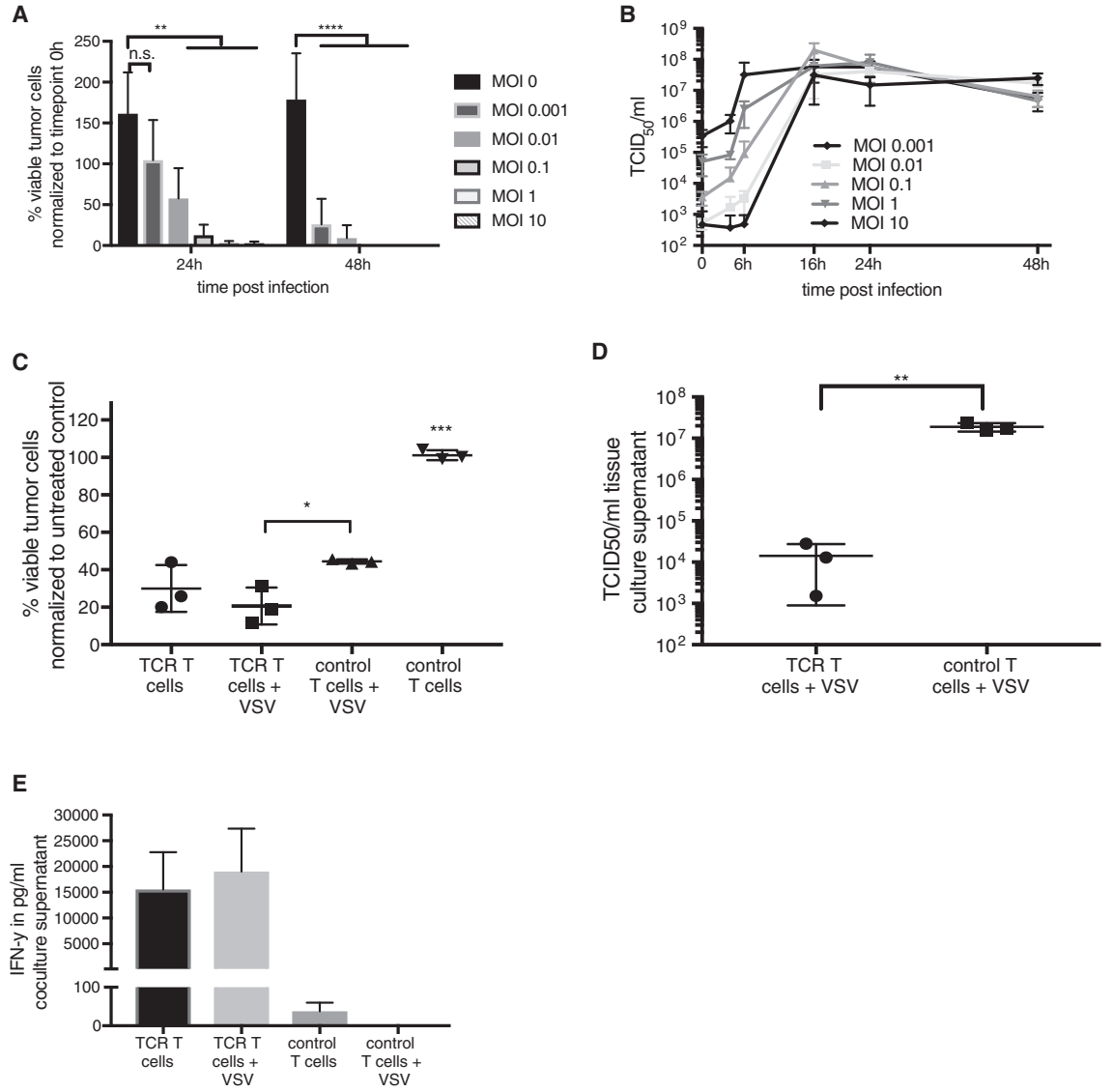

Figure 3. ML2B7-Fluc Leukemia Cells Are Susceptible to Treatment with VSV and CD8⁺ T cm

ML2B7-Fluc cells were infected with indicated MOIs of rVSV-tk. (A) Cell viability was assayed by measuring the luciferase activity of viable tumor cells. The means ± SD from three independent experiments, performed in triplicates, are shown. Two-way ANOVA with Bonferroni post-test was performed to determine statistical significance (**$p < 0.01$; ****$p < 0.0001$). (B) Virus titers in culture supernatants at the indicated time points were assayed by $TCID_{50}$. Means ± SD from three individual experiments, performed in triplicates, are shown. (C) Luciferase assays were performed to determine the number of viable ML2B7-Fluc tumor cells 24 hr after treatment with indicated treatment groups. TCR transduced and control T cells were uninfected or infected with rVSV-tk at an MOI of 0.1 before being added in a 1:20 ratio to the tumor cells. Individual replicates and means ± SD from three experiments performed in triplicates from three different T cell donors are shown. The percentage of living cells was normalized to untreated control cells. One-way ANOVA with Bonferroni post-test was performed (*$p < 0.05$; ***$p < 0.001$). (D) Viral titers from co-culture supernatants were measured by $TCID_{50}$. Individual replicates and means ± SD are shown. Statistical analysis was performed using unpaired t test (**$p < 0.01$). (E) IFN-γ concentrations in coculture supernatants were measured by ELISA assay. Means ± SD are shown.

subsequent efficacy studies, we decided to use the dose at which no toxicity was observed within the first 14-days post-treatment, which was 10^4 PFU. No observable toxicity for up to 21 days was observed in mice treated with 10^7 $CD8^+$ T cm infected at an MOI of 0.1, which corresponds to an actual transferrable dose of 4.2×10^4 PFU. These doses were applied in all subsequent experiments. Although a long-term safe dose of naked VSV could not be determined from this experiment, we can conclude that the MTD of VSV over the 21-day monitoring period could be elevated by more than 4-fold by loading the virus onto carrier T cells.

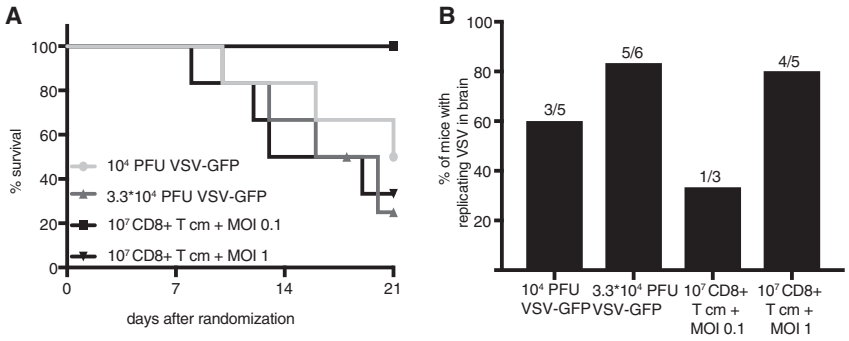

Figure 4. Loading of VSV onto T cm Reduces Virus Toxicity in NSG Mice

(A) Increasing doses of naked rVSV vectors expressing GFP or rVSV vectors expressing GFP loaded onto $CD8^+$ T cm were injected by tail-vein injection in NSG mice (n = 3–6). Mice were followed for up to 21 days and then censored. Kaplan-Meier survival curves are shown. The virus dose that was loaded onto T cells was calculated using the equation derived from Figure 2. (B) $TCID_{50}$ assays were performed on homogenized brain tissue. The percentage of mice that had a replication-competent virus in the brain is shown (10^4 PFU VSV-GFP: n = 5; $3.3*10^4$ PFU VSV-GFP: n = 6; 10^7 $CD8^+$ T cm, MOI 0.1 of VSV-GFP: n = 3; 10^7 $CD8^+$ T cm, MOI 1 of VSV-GFP: n = 5). Brains were collected upon euthanasia at the time point of toxic events or at the end of the 21-day monitoring period.

TCR $CD8^+$ T cm Accumulate Specifically in Target Tumors and Deliver Virus More Efficiently Than Systemically Applied Naked Virus

To test TCR T cell homing and viral delivery *in vivo*, we implanted subcutaneous ML2B7 into the flanks of NSG mice (Figure S2). Investigation of intratumoral accumulation of $CD8^+$ T cells after the indicated therapy regimen was performed by flow cytometry analysis of tumors at 5 days post-treatment (Figure 5A). Dead cells were excluded from analysis. Although T cell infiltration was low at early time points (days 1 and 3) after treatment, regardless of TCR transduction (data not shown), a specific accumulation of TCR T cells was observed on day 5 in mice that were treated with the TCR T cells or the combination of TCR T cells and VSV, indicative of specific activation and proliferation of the TCR T cells in the presence of their target antigen (Figure S3). Although there was a slight increase in intratumoral infiltration of TCR T cells in the mice treated with uninfected TCR T cells, this difference was not significant compared with the combination, indicating that VSV infection does not impair TCR T cell activation or expansion *in vivo*. Almost no infiltration was observed for tumors of mice that had been treated with control T cells. These data are consistent with immunohistochemical staining for human CD3 from tumor tissue obtained on day 5 post-treatment, which demonstrated positivity only in tumors treated with TCR T cells (Figure 5C). Intratumoral viral titers were measured by $TCID_{50}$ for determination of delivery efficiency (Figure 5B). High viral titers reaching more than 10^6 $TCID_{50}$/mg tumor at 72 hr post-injection were detected within tumors of mice treated with VSV delivered via carrier cells, whereas VSV monotherapy resulted in titers approximately 1-log lower at the same time point. These data indicate that T cm are effective carrier cells for delivery and allow for enhanced tumor transduction efficiency of systemically applied oncolytic VSV.

Combination of T Cells with VSV Causes Rapid Tumor Necrosis

A comparison of treatment efficacy in ML2B7 tumors was performed by analyzing the percentage of viable GFP^+ tumor cells after exclusion of dead cells by flow cytometry (Figure 6A). The combination of T cells with VSV, regardless of TCR transduction, led to a more rapid and reproducible decrease of viable tumor cells compared with other treatment groups at 120 hr after beginning therapy, which was further confirmed by histological quantification of tumor necrosis (Figure 6B). Representative images of tumor histology are shown in Figure 6C. The mice treated with naked VSV also showed a loss in tumor viability; however, this effect was highly variable, which we attribute to the relatively low tumor transduction efficiency of non-shielded VSV applied by systemic administration. ML2B7 tumor rejection was observed within several days after treatment with combination therapies or with uninfected TCR T cells (Figure 6D). Complete rejection of ML2B7 tumors was observed as early as 7 days post-treatment in those mice treated with TCR T cm. Although the combination therapy resulted in a delayed reduction of tumor size, histological and FACS analysis indicate an extremely rapid and reproducible cytotoxic effect, which was significantly enhanced compared with VSV monotherapy. Interestingly, the difference in tumor size on day 10 after therapy was not significant between TCR T cells monotherapy and both combination therapies; however, it should be noted that tumor size is not necessarily a reflection of tumor viability, especially in the absence of inflammatory cells for clearance of dead tissue. Furthermore, we hypothesize that the multi-faceted benefits of the combination therapy can only be truly appreciated in an immune-competent system.

Immune Escape Leads to Tumor Relapse following T cm Monotherapy

A survival study as a parameter for overall efficacy was conducted in ML2B7 tumor-bearing mice. Because of the immune deficiency of the NSG mice, we could not extract meaningful survival data for the groups receiving VSV, because those mice died due to viral-induced toxicity, rather than tumor burden. TCR T cell therapy compared with control T cells or PBS showed a substantial survival advantage (Figure 7A). However, despite the initial tumor clearance in the TCR group, all but one mouse experienced relapse over the total observation period of 90 days (Figure 7B). Although TCR T cell monotherapy was re-administered on day 52 after initial therapy (indicated by the line), the tumors continued to grow in four out of five mice. Upon euthanization, the relapsed tumors were analyzed by flow cytometry (Figure 7C). None of the refractory relapsed tumors expressed the transduced HLA-B*07:02 linked to EGFP, as demonstrated in the representative dot plot on the right side. For

Table 1. Testing of Different Doses of Free and Cell-Bound VSV in an MTD Study in NSG Mice

Treatment	Corresponds to	Toxic Events within 21 Days
10^4 PFU VSV-GFP	10^4 PFU	3/6
3.3×10^4 PFU VSV-GFP	3.3×10^4 PFU	4/6
10^7 CD8$^+$ T cm, MOI 0.1	4.2×10^4 PFU	0/3
10^7 CD8$^+$ T cm, MOI 1	5.2×10^5 PFU	4/6

According to the equation derived in Figure 2, the applied doses of naked and T cm-associated virus units are shown, as well as the absolute number of toxic events and number of mice used for each treatment group.

reference, a control tumor with GFP expression is shown on the left. The long-term surviving mouse had no detectable tumor remaining for analysis. Whether the relapsed tumors were the result of HLA loss or of outgrowth of a minor percentage of implanted untransduced tumor cells is difficult to speculate. However, this experiment highlights the fact that, although TCR T cells are a powerful tool for treatment of leukemia tumors, as monotherapies, they are limited in that they target only one specific antigen presented on a certain HLA, and they will fail when tumors are heterogeneous or undergo immune-escape mechanisms such as HLA-downregulation or antigen loss. This argues for the benefit of a combination with oncolytic virus therapy, because the viral-mediated cytopathic effects are independent of antigen expression.

DISCUSSION

Following the US Food and Drug Administration (FDA) approval of oncolytic herpes simplex virus-based T-Vec (Imlygic) in 2015, and the recent approval of CD19-targeted chimeric antigen receptor (CAR) T cells (Kymriah) for patients with acute lymphoblastic leukemia (ALL), the field of immune-oncology is now in the spotlight, and the enthusiasm for the use of oncolytic viruses is at a peak. Although there has already been a report describing the use of carrier T cells for delivery of rVSV-ΔM51,[18] our study is, to our knowledge, the first to perform such a combination therapy using human T cells together with wild-type VSV *in vivo*. We could show that T cells not only provide viral amplification, but they can also shield VSV from neutralizing antibodies, and furthermore, we clearly demonstrate, in this proof-of-principle study, that the combination is effective both in tumor cell killing and in improving the safety of systemic VSV therapy.

In our first experiments we demonstrate that T cells are able to support viral replication, as well as shield VSV from neutralization. Considering that VSV is an oncolytic virus with cancer cell selectivity, the fact that VSV replicated in T cells might be alarming. However, it was previously shown that VSV replication in T cells is cell cycle dependent.[34] Because the T cells used in our study were activated and in a highly proliferative state, this would provide a mechanism for permitting VSV replication. Furthermore, our observations indicated virus replication and transgene expression seemed to be limited to clusters of proliferating cells, as determined by fluorescence microscopy (data not shown), and not nearly to the same extent as in ML2 tumor cells. It was also demonstrated that 48 hr after infection, there was still a considerable percentage of viable T cells. Further investigations are needed to determine whether this is due to a minor population of generally resistant T cells that start to outgrow the sensitive T cells, or whether the T cells initiate an antiviral defense system, which limits the ability of the virus to replicate in those protected cells.

Concordant with the findings above, cell viability of the central memory compartment of CD8$^+$ T cells was not strongly impaired after virus infection, although there was a dose-responsive cell killing. In light of increasing titers at early time points after infection, despite low infection efficiency, we conclude that an infection of a small percentage of CD8$^+$ T cm is sufficient to produce a high viral output. This suggests that VSV-loaded CD8$^+$ T cm could be a promising combination therapy, because we achieved high viral transfer to the tumor without significantly impairing the number of functional tumor-reactive T cells. As previously reported for mouse T cells,[18] we have also demonstrated that the human CD8$^+$ T cm can not only internalize VSV, but also carry VSV on their surface, which is rapidly transferred to other cells. We hypothesize that carrying infectious virus both internally and externally provides a complementary mechanism: the externally loaded virus could be transferred to the tumor without compromising the effector function of the T cell, whereas the internalized virus would allow expansion of the input dose. At very early time points (4 hr) post-infection, we actually observe a slight decrease of infectious virus in our CD8$^+$ T cm culture, which could be caused by virions that were initially only loosely associated with the cell membrane and entered the T cells in the absence of other cell recipients (i.e., tumor cells). Together, these data strongly support the hypothesis that CD8$^+$ T cm can efficiently amplify and deliver VSV to other cells.

In Figure 3 we can explore whether a combination of T cells and VSV can enhance tumor cell killing compared with VSV monotherapy. In making such a comparison, it is necessary to consider that the amount of virus directly added to the tumor cells will be quite different from if an equivalent amount is added via infection of T cells at the same MOI. In order to estimate the amount of virus transferred via T cells, we can apply the equation derived in Figure 2. This calculation indicates an applied dose of only 21 PFU for 10^5 tumor cells, which is the equivalent of an MOI of 0.00021. Impressively, if we compare the reduction in tumor cell viability achieved with this scant amount of virus administered via T cm, it is substantially greater than the effects of naked VSV application, even when administered at an MOI of 0.001 (five times the amount applied in the combination). Here, it has to be taken into consideration that the T cells will also support VSV replication, and in so doing, they will amplify the amount of VSV available to kill ML2 tumor cells. This highlights the synergistic potential of a combinatorial approach. The fact that a combination of TCR T cells with VSV is superior to the combination of control T cell with VSV *in vitro* also supports the concept that the two anticancer agents synergize. Even though we can only report a trend toward better therapeutic efficacy from the VSV-infected TCR T cells compared with uninfected TCR T cells, we suggest that in this artificial setting, in

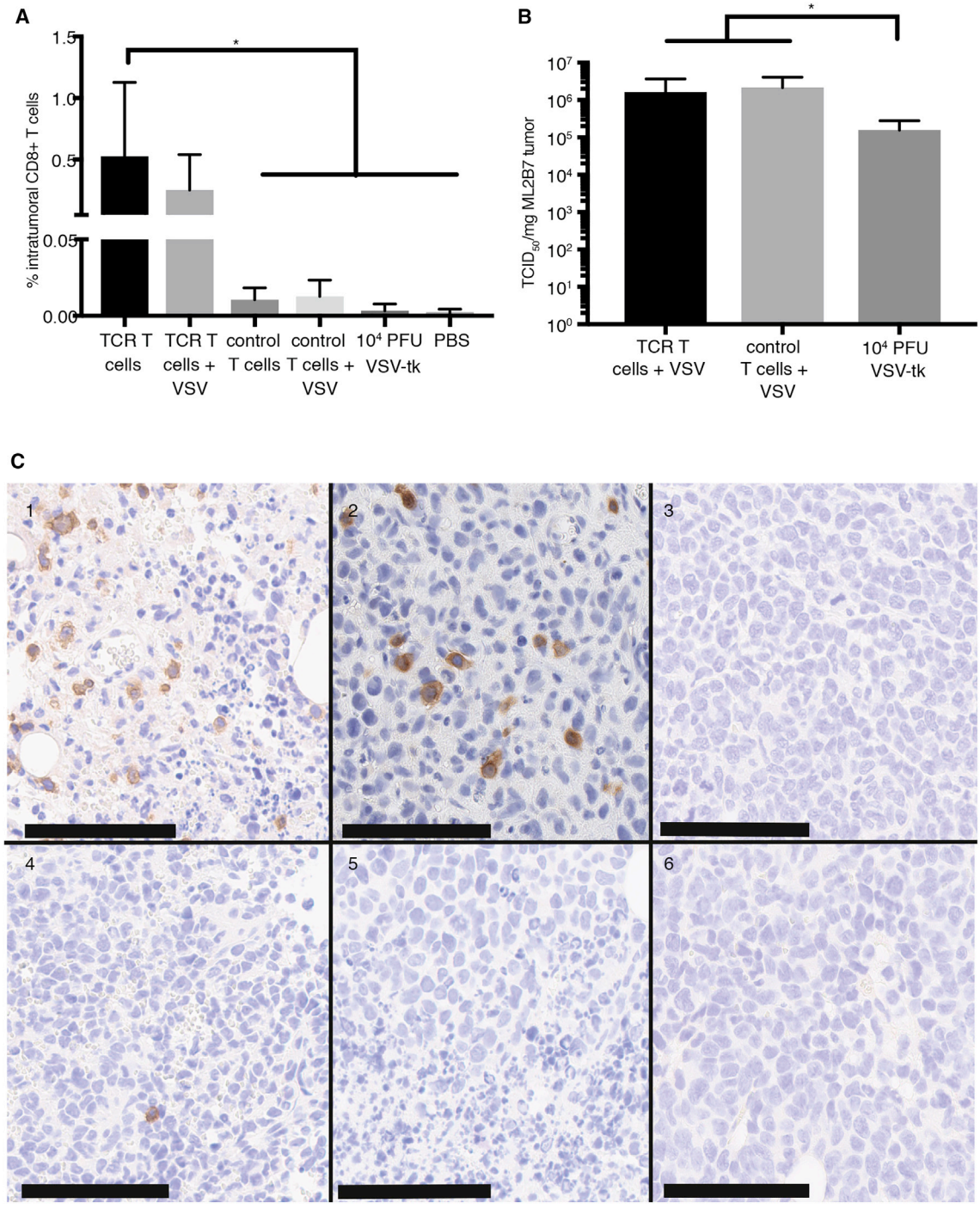

Figure 5. TCR CD8⁺ T cm Deliver Virus to the Tumor and Proliferate Specifically in Target ML2B7 Cells

Tumor-bearing NSG mice were treated systemically with the indicated T cells and/or rVSV-tk and euthanized after 120 hr. (A) The percentages of intratumoral $CD8^+$ T cells was determined by FACS analysis. *The p value for the TCR T cell group compared with PBS, 10^4 PFU VSV-tk, and control T cells after 120 hr is <0.05, as determined by one-way ANOVA with Bonferroni post-test. Means ± SD are shown (n = 3–5). (B) Intratumoral viral titers at 72 hr post-treatment were measured by $TCID_{50}$ analysis of tumor homogenates. Means ± SD are shown. Statistical analysis was performed by Mann-Whitney test (*$p < 0.05$; n = 4–6). (C) Immunohistochemical staining for $CD3^+$ cells in tumor tissue at 120 hr post-treatment was performed. Representative images are shown: 1, TCR T cells; 2, TCR T cells infected with rVSV-tk at MOI 0.1; 3, 10^4 PFU rVSV-tk; 4, control T cells; 5, control T cells infected with rVSV-tk at MOI 0.1; 6, PBS. Scale bars indicate 100 μm.

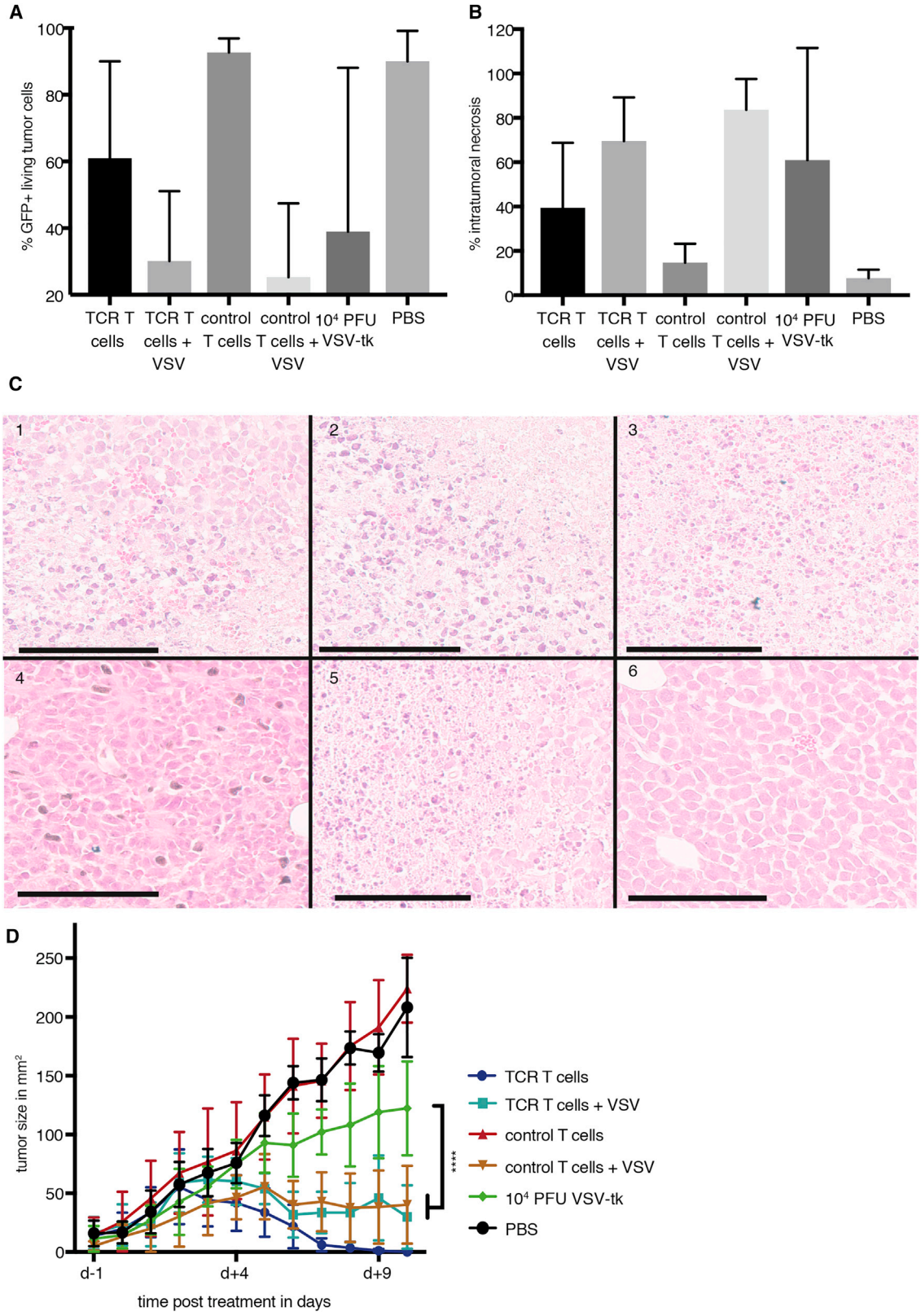

(legend on next page)

which T cells and tumor cells are forced in close proximity, tumor cells have high target antigen presentation, and there are no other factors that interfere with T cell effector function, the effect of the TCR T cells is easily overestimated. We therefore believe that, in a clinical setting with a highly immune-suppressive microenvironment and heterogenous antigen presentation, the advantage of VSV-loaded TCR T cells compared with the cell therapy alone would be more easily appreciated.

Contradictory to the enhanced efficacy of VSV delivered via T cm were the reduced viral titers achieved when TCR T cells were co-cultured with their target tumor cells; however, the T cell-mediated tumor cell killing leads to a reduction of tumor substrate to serve as host for virus replication. Furthermore, IFN-γ, which is produced by the T cells upon activation by their target cells, is known to elicit antiviral activity to inhibit VSV, although not nearly to the same extent as the type I IFNs,[35] which might be another mechanism leading to reduced viral titers when compared with control T cells. Regardless, reduced viral titers in this setting have the advantage of providing a safety mechanism to prevent the onset of viremia, because efficient tumor cell killing was observed without the need for high viral titers. Indeed, we observed reduced toxicity in our mouse model when we applied VSV via infected $CD8^+$ T cm. We speculate that the internalization of VSV by the T cells, as well as the slow release that likely results in very different pharmacokinetics than an intravenously administered bolus of naked virus, contribute to the improved safety. Another possible explanation is that human T cells preferentially home to lungs and spleen in NSG mice,[30] where they release the virus to non-permissive cells, thereby reducing the amount of circulating virus and potentially preventing off-target effects. Regardless of the mechanism for the improved safety of oncolytic VSV therapy in combination with T cells as carrier cells, the substantial reduction in toxicity is a compelling benefit of the combination therapy.

In spite of the potential reduction of bio-available virus by T cell internalization, we demonstrate an enrichment of replicating VSV in the tumors of mice treated with a combination of VSV and T cells. Interestingly, at early time points after therapy, we observed very few $CD8^+$ T cells in the tumors, regardless of transduction with the TCR (data not shown). We speculate that the accumulation of virus within the tumor is due to the transfer from randomly infiltrating, rather than specifically homing, T cells. Nevertheless, it seems that those few infiltrating T cells are still more efficient at delivering virus than intravenous administration of naked VSV. Moreover, we observe a specific increase of TCR T cm in the tumor at later time points, indicating that, upon arrival at the tumor, they recognize their antigen and begin expansion. Also, an important point concerning the lower intratumoral viral titers and the highly variable responses to VSV monotherapy is that the delivery of "naked" VSV to tumors via systemic administration is a random and inefficient process. The majority of the injected dose is subject to inactivation by blood components or filtration by the liver and spleen, leaving only a small percentage of the applied virus dose available to reach and infect the tumor. This mechanism is most likely responsible for the high degree of variation in tumor killing by VSV monotherapy that we observed in this study. The application of VSV via carriage on T cells, on the other hand, allows for protection and amplification of the internalized virions, as well as the ability to inject higher virus doses due to the improved safety, all of which can combine to result in the enhanced tumor transduction and response compared with VSV monotherapy.

Surprisingly, the use of control T cells was equally as efficient in treating the tumor in combination with VSV as TCR T cells. It seems that the initial viral delivery rather than the transduction status of the T cells is a predictor for treatment efficacy. Monitoring of tumor size over time revealed that the combination of T cells with virus was significantly more effective than VSV alone at inhibiting tumor growth. In an immune-competent system, we would expect an even bigger advantage of the combination therapy, due to faster neutralization of naked virions by the innate and adaptive anti-viral responses. In our model system, the tumor rejection kinetics demonstrates that TCR T cells alone are sufficient to clear the ML2B7 tumor faster than any other therapy group; however, we do not view this as contradictory to our other data nor our central hypothesis. As previously mentioned, a critical point in this setting is that the T cells will efficiently recognize their antigen in the homogenously transduced tumor cells.[29] In a clinical setting, the TCR T cells alone would face more hurdles to clear a tumor with heterogenous antigen expression and antigen loss,[36] drift, and shift.[37,38]

Despite the prolonged survival afforded by TCR T cell monotherapy, our study highlights the limitation of adoptive T cell therapy, in which therapy-resistant tumor cells, caused by HLA loss or an outgrowth of non-transduced tumor cells, result in eventual relapse. This underscores the benefit of the combination therapy, because VSV has the capacity to kill every tumor cell, irrespective of antigen expression, and further could mediate additional responses to broaden the immune-mediated effect of adoptively transferred T cells.[7] Furthermore,

Figure 6. Treatment with TCR $CD8^+$ T cm Loaded with VSV Causes Rapid Necrosis in ML2B7 Tumors

NSG mice bearing ML2B7 tumors were treated by tail-vein injection with T cells and/or rVSV-tk as indicated. (A) The percentage of GFP^+ tumor cells at the indicated time points was determined by flow cytometry after exclusion of dead cells by staining with Viobility 405/520 fixable dye. Mean ± SD are shown (n = 3–5). (B) Tumor sections from mice euthanized at the indicated time points were analyzed histologically for quantification of necrosis. Three individual sections of each tumor were analyzed. Mean ± SD are shown (n = 3–6). (C) Representative histological images from each treatment group are shown: 1, TCR T cells; 2, TCR T cells infected with rVSV-tk at MOI 0.1; 3, 10^4 PFU rVSV-tk; 4, control T cells; 5, control T cells infected with rVSV-tk at MOI 0.1; 6, PBS. Scale bars indicate 100 μm. (D) Tumor sizes were measured daily with a caliper until day 10 after therapy was started. Tumor area is expressed as mean ± SD (n = 4–6). Two-way ANOVA with Bonferroni post-test was performed (****$p < 0.0001$). PBS and control T cell groups were not significantly different from each other. They were both significantly (****) different from all other groups. The TCR T cell group was significantly (****) different from the VSV therapy group.

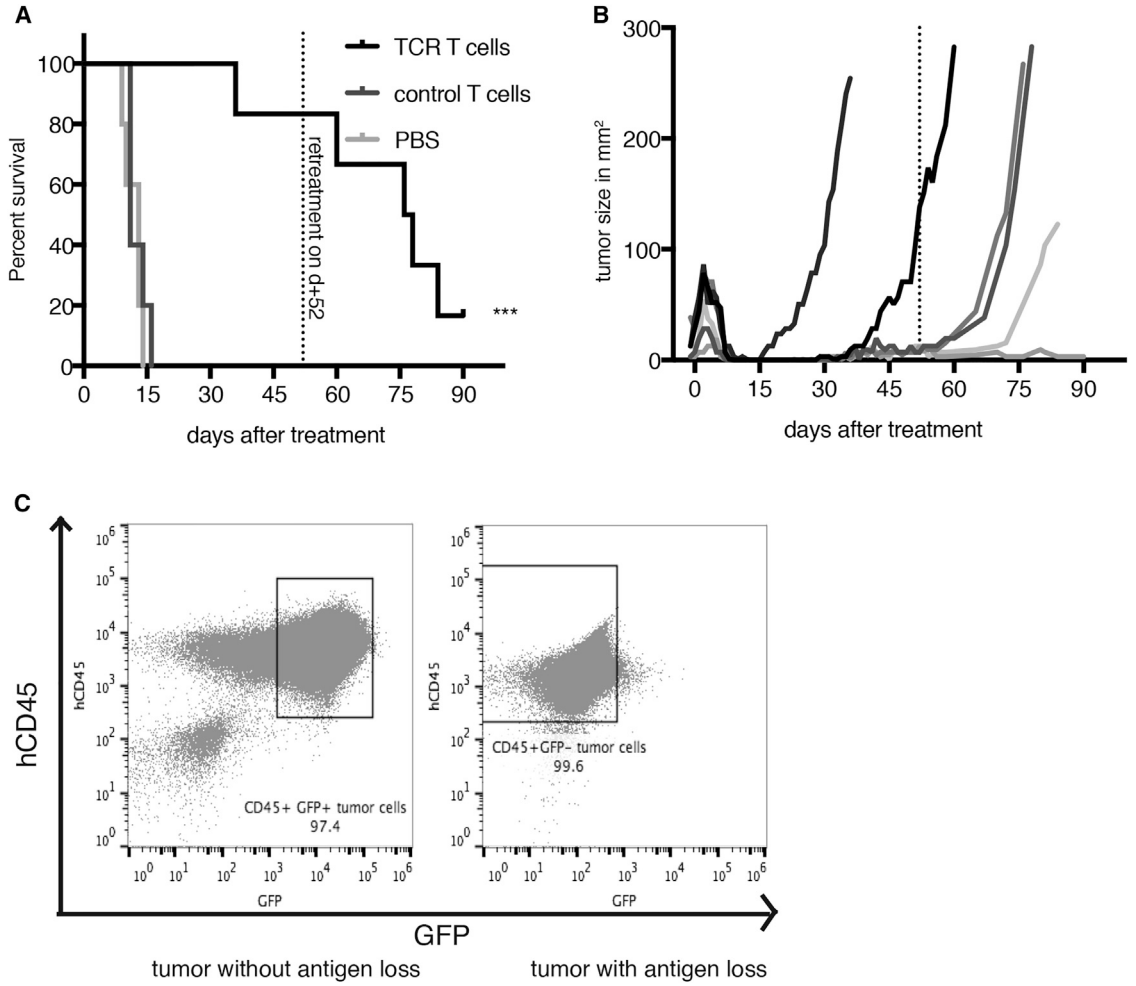

Figure 7. TCR CD8⁺ T cm Monotherapy Leads to Tumor Relapse in Target ML2B7 Tumors in NSG Mice

ML2B7 tumor-bearing NSG mice were treated 10 days after tumor implantation by tail-vein injection and were euthanized at humane endpoints due to poor health or when the tumors reached a diameter of 2 cm. (A) Survival times were plotted by Kaplan-Meier curve (n = 5–6). Long-term surviving TCR T cell-treated mice with relapsing tumors were administered a second round of treatment on day 52 after initial therapy as indicated. ***p < 0.0001 by log-rank [Mantel-Cox] test. (B) Tumor sizes of individual mice treated with TCR T cells were plotted until the time of euthanasia. The dotted line indicates the time point of the second treatment with TCR T cells. (C) Relapsed tumors were analyzed by flow cytometry to determine presence of the targeted HLA, using the co-expressed GFP as a surrogate marker. Representative FACS dot plots of control tumor that expressed the HLA (left) and a relapsed tumor lacking GFP expression (right) are shown.

in an immune-competent model, we would expect the induction of a polyclonal antitumor immune response mediated by VSV.[7] Finally, it is important to note that tumor size is not always indicative of therapy response, especially because NSG mice lack the inflammatory tools, such as functional monocytes and dendritic cells,[39] to efficiently clear dead tissue.[40,41] Therefore, the fact that there were still palpable tumors in the combination treatment group does not necessarily indicate that those small tumors were viable. In fact, FACS and necrosis analysis indicated that there were very few viable tumor cells in tumors of mice treated with one of the combination therapies.

A limitation of the immune-deficient NSG model is the sensitivity to replicating viruses, thereby preventing us from conducting a meaningful survival analysis, because the VSV-treated mice generally succumbed to virus toxicity. Although VSV continues to be intensively explored as a promising oncolytic virotherapeutic, it is well recognized that wild-type VSV is far too toxic, even in immune-competent hosts, to have a realistic future in clinical application. For this reason, we and others have engineered recombinant forms of VSV that are substantially safer than the wild-type.[42–44] In the current study, we have used VSV vectors based on a wild-type backbone to serve as a representative of this OV platform. Due to the severe neurotoxicity elicited by this VSV vector in the immune-suppressed host, we were able to demonstrate a clear enhancement of safety by loading the virus onto T cells for systemic delivery. However, for further development toward clinical translation, we would propose to adapt

the therapy to employ one of the VSV vectors that have demonstrated improved safety profiles.

A key finding of this investigation was that human TCR T cells as carriers of VSV represent a powerful approach to improving the safety and efficacy of systemically applied virus, which have been major challenges in the clinical translation of oncolytic VSV therapy. Even though TCR T cells on their own were extremely effective in this model, they eventually failed because of the realistic phenomenon of tumor immune escape. This highlights the need for a multi-modal and broader immune therapy, which can be accomplished by oncolytic virus therapy. In an immune-competent model, the potential onset of a VSV-mediated antitumor polyclonal immune response could provide an elegant mechanism to address the challenge of immune evasion. Unfortunately, the establishment of a human immune system in NSG mice is limited by graft-versus-host disease,[45] limiting the possibility of testing human cell therapies in an immune-competent setting in preclinical rodent models. Advances in the generation of "humanized" mouse models will soon enable us to test human adoptive cell therapies in a more translational setting.

In conclusion, although additional investigations in more clinically relevant models are warranted, this study provides a compelling proof-of-principle of the potential of human T cells as carriers and synergistic effector cells to substantially enhance the safety and efficacy of oncolytic VSV, resulting in an optimal and rationally designed cancer therapeutic. Due to the direct oncolytic effect of VSV, coupled with the potential of VSV to mediate potent and systemic antitumor immune responses, it represents an ideal virus to incorporate into immuno-therapeutic cancer strategies. $CD8^+$ T cm are ideal carrier cells for safely delivering higher doses of VSV systemically and imparting potent antitumor effector functions. This approach will be further developed in subsequent studies in anticipation of the potential clinical translation as a combined viro-immunotherapeutic for cancer.

MATERIALS AND METHODS

Isolation and Enrichment of Primary Human T Cell Populations

Blood was collected from human volunteers according to the principles of the Declaration of Helsinki and the local ethics committee. Peripheral blood mononuclear cells (PBMCs) were prepared from blood via separation on Ficoll gradients as described previously.[30,31] $CD8^+$ T central memory cells ($CD8^+$ T cm) were enriched in a first step by magnetic positive separation of $CD8^+$ T cells (Miltenyi Biotec, Bergisch Gladbach, Germany) or by negative selection of $CD8^+$ memory T cells using the MagniSort Human CD8 Memory T cell Enrichment Kit (Thermo Fisher Scientific, Waltham, MA, USA), followed by enrichment by flow cytometry for cellular expression of CD62L and CD45RO.

Cell Lines and Cell Culture

Primary human T cells, ML2 cells (the CABRI consortium), and BHK-21 cells (ATCC) were cultured as described previously.[22,30,31] 293Vec-RD114 (BioVec Pharma, Québec, Canada) cells were cultured in DMEM (Thermo Fisher Scientific, Waltham, MA, USA) supplemented with 10% FBS, 10 mM non-essential amino acids, 100 IU/mL penicillin-streptomycin, sodium pyruvate, and 2 mM L-glutamine. Cells were checked regularly by microscopy, and mycoplasma contamination was tested routinely. T cells used in experiments were between 2 and 4 weeks old.

Coculture assays of ML2B7-Fluc tumor cells and T cells were performed in T cell medium. Directly after infection and washing of T cells they were added to the ML2B7-Fluc tumor cells in a 1:20 ratio (effector:target). Viability of ML2B7-Fluc cells was measured by luciferase activity as described below.

Viral Transduction

Retroviral transduction of human T cells with iRFP or the TCR2.5D6[29] linked to iRFP was performed as described previously.[29–31] ML2 cells were transduced to express the HLA-B*07:02 linked to EGFP (ML2B7),[30,31] or the HLA-B*07:02 linked to EGFP and Firefly-luciferase (ML2B7-Fluc). Transduced cells were sorted and cloned by limiting dilution to generate stable cell lines expressing the respective transgene, as described previously.[30,31] Transgene expression was tested regularly by flow cytometry.

Recombinant Viruses

rVSV vectors expressing GFP,[46] an enhanced version of the herpes simplex thymidine kinase (rVSV-tk),[22] or firefly luciferase (rVSV-Luc) were produced as described previously.[22,46] All rVSV vectors were based on the wild-type VSV Indiana backbone, with no mutations in the matrix (M) protein. Titers of viral stocks were determined by standard plaque assays as described before for determination of vial titers.[22,46] Viral titers in experimental samples were measured by 50% tissue culture infectious dose assay ($TCID_{50}$) in BHK-21 cells as previously described[22] following the Reed-Muench method. MOI is given as PFU per cell. From homogenized tissue as few as around 10^1 $TCID_{50}$/mg tissue could be detected.

Viral Infection of T Cells and Tumor Cells

Cell suspensions with a concentration of 4×10^6 cells/mL in DPBS containing Ca^{2+} and Mg^{2+} (PAN-Biotech, Aidenbach, Germany) were infected with VSV at the indicated MOI. Following a 1-hr infection at room temperature, the cells were washed three times prior to proceeding with experiments.

Cell Viability Assays

Cell viability of $CD8^+$ T cm was determined by trypan blue assay. During experiments, the amount of viable cells was determined by counting them in a Neubauer-Chamber. Percentage of living cells was normalized to time point 0 hr. Cell viability of ML2B7-Fluc tumor cells was measured as a function of luciferase activity using the Dual-Luciferase Reporter Assay System according to the manufacturer's instructions (Promega, Madison, WI, USA). In brief, at the indicated time points, tumor cells were washed to remove remnants of dead cells and subsequently lysed before luciferase activity of tumor cells could be measured in a luminometer.

Flow Cytometry

Flow cytometric analysis of experiments was performed on a Gallios Flow Cytometer (Beckmann Coulter, Brea, CA, USA). Antibodies used for $CD8^+$ T cm enrichment were: CD62L-phycoerythrin (PE) (clone: 145/15; Miltenyi, Bergisch-Gladbach, Germany), CD45RO-PE-Vio770 (clone: UCHL1; Miltenyi), and propidium iodide (PI) (Thermo Fisher Scientific, Waltham, MA, USA). For flow cytometric analysis the following antibodies were used: CD3-PE-Vio615 (clone: REA613; Miltenyi), CD8-peridinin chlorophyll protein complex (PerCP)-Vio700 (clone: BW 135/80; Miltenyi), CD8-VioGreen (clone: BW 135/80; Miltenyi), and CD45-V450 (clone: HI30) (BD Biosciences). Live/dead cell discrimination was performed with 7-AAD (Sigma-Aldrich, St. Louis, MO, USA) and Viobility 405/520 Fixable Dye (Miltenyi). Cell doublets were excluded from analysis.

Calculation of Transferrable Amount of VSV

After infection of $CD8^+$ T cm with indicated MOIs of rVSV vectors expressing GFP following the described standard procedure and washing steps, they were added in a 1:10 ratio to BHK-21 cells and co-cultured for 6 hr. Afterward, the supernatant was removed, and the BHK-21 monolayers were washed and trypsinized. By removing the medium and washing the BHK-21 cells, all suspension T cells should be removed. To exclude remaining contamination of BHK-21 cells with T cells, dead cells and remaining T cells were excluded from analysis by 7-AAD and CD3 staining. The percentage of GFP^+ BHK-21 cells was determined by FACS and used as surrogate parameter for the amount of virus that was transferred from T cells to BHK-21 cells. Afterward, the amount of transferred virus was calculated and used to determine the amount of virus that was associated with T cells before being transferred to the BHK-21 cells.

Antibody-Protection Assay

To determine whether T cells would protect VSV from antibody-mediated neutralization, 10^6 T cells were infected with rVSV-Luc at an MOI of 10, as described before. After extensive washing steps, the virus-loaded T cells or 10^7 PFU of "naked" rVSV were incubated in PBS, control serum, or serum from rats that had been immunized with VSV, for 90 min at 37°C. After washing, cells were lysed by two freezing and thawing cycles to allow for quantification of internalized and free virus. Viral titers from lysate or naked VSV were measured by $TCID_{50}$ assay.

IFN-γ ELISA

IFN-γ ELISA was performed from tissue culture supernatants from indicated conditions using the BD OptEIA Human IFN-γ ELISA Set (BD Biosciences) according to the manufacturer's instructions.

Animal Studies

Animal studies were performed in accordance with authorization by the local government and institutional guidelines. NSG (The Jackson Laboratory, Bar Harbor, ME, USA) mice were injected subcutaneously with 10^7 ML2B7 tumor cells on the right flank (Figure S1). Tumor size was measured using a caliper. Mice were treated intravenously (tail vein) on day 11 after tumor implantation for kinetic studies and day 10 for survival and tumor rejection studies. Tumor-bearing mice that received T cells were additionally administered 1 μg of interleukin-15 (IL-15; Miltenyi) weekly by intraperitoneal injection. To determine the MTD, we followed the standard 3+3 Fibonacci dose escalation scheme used in clinical dose-finding investigations.[47] Three mice per group were subjected to the indicated doses of VSV and monitored for 21 days for signs of toxicity. If no toxicity was observed, the next higher dose was tested. If a single toxic event was observed, three additional mice were added to this dose level. If no toxic event was then observed, the dose was considered safe. Toxicity was defined as significant weight loss, obvious signs of general sickness, or neurotoxicity.

Further details and the exact numbers of mice per group for each experiment are outlined in the Supplemental Information (Figure S2; Tables S1–S5).

Histology, Necrosis Quantification, and Immunohistochemistry

Tissues were processed by standard procedures for fixation, dehydration, and paraffin embedding, prior to being cut into 2-μm sections. Standard H&E staining was performed on three different regions of the tumor separated by approximately 150 μm. The degree of necrosis was quantified using the Aperio ImageScope Software (Leica Biosystems, Nussloch, Germany) after scanning the slides. Immunohistochemistry (IHC) for CD3 was performed as described previously.[30,31]

Statistical Analysis

Data are shown as mean ± SD, unless otherwise indicated. Data were analyzed using GraphPad Prism. Statistical analyses were performed as indicated in the figures.

SUPPLEMENTAL INFORMATION

Supplemental Information includes three figures and five tables and can be found with this article online at https://doi.org/10.1016/j.omto.2018.12.001.

AUTHOR CONTRIBUTIONS

Conception and Design: M.K.M., S.M., O.E., A.K., and J.A. Development of Methodology: M.K.M., L.Z., S.M., and J.A. Acquisition of Data (provided animals, acquired and managed patients, provided facilities, etc.): M.K.M., L.Z., S.M., K.S., and J.A. Analysis and Interpretation of Data (e.g., statistical analysis, biostatistics, computational analysis): M.K.M., L.Z., S.M., K.S., O.E., A.K., and J.A. Writing, Review, and/or Revision of the Manuscript: M.K.M., S.M., O.E., A.K., and J.A. Administrative, Technical, or Material Support (i.e., reporting or organizing data, constructing databases): M.K.M., K.S., R.M.S., O.E., A.K., and J.A. Study Supervision: O.E., A.K., and J.A.

CONFLICTS OF INTEREST

The authors declare no competing interests.

ACKNOWLEDGMENTS

The authors thank Olga Seelbach, Marion Mielke, Stefanie Rämisch, Markus Utzt, and Sebastian Blaschke for excellent technical support.

Cell sorting on the BD FACSAria III was supported by the DKTK cell sort facility in the department of Jürgen Ruland. Cell sorting on the Sony SH800 was supported by Bastian Höchst. We want to thank Henrique Bianchi for preparing the ML2B7-FLuc cell line, as well for taking care of animal breeding. This work was supported by grants from the Deutsche Forschungsgesellschaft (SFB824 subproject C7 to J.A., SFB824 subproject C10 to A.K., SFB824 subproject Z3 to K.S.).

REFERENCES

1. Chen, Y., Pan, Y., Guo, Y., Zhao, W., Ho, W.T., Wang, J., Xu, M., Yang, F.C., and Zhao, Z.J. (2017). Tyrosine kinase inhibitors targeting FLT3 in the treatment of acute myeloid leukemia. Stem Cell Investig. *4*, 48.
2. O'Donnell, M.R., Tallman, M.S., Abboud, C.N., Altman, J.K., Appelbaum, F.R., Arber, D.A., Bhatt, V., Bixby, D., Blum, W., Coutre, S.E., et al. (2017). Acute myeloid leukemia, version 3.2017, NCCN Clinical Practice Guidelines in Oncology. J. Natl. Compr. Canc. Netw. *15*, 926–957.
3. Döhner, H., Weisdorf, D.J., and Bloomfield, C.D. (2015). Acute myeloid leukemia. N. Engl. J. Med. *373*, 1136–1152.
4. Gbolahan, O.B., Zeidan, A.M., Stahl, M., Abu Zaid, M., Farag, S., Paczesny, S., and Konig, H. (2017). Immunotherapeutic concepts to target acute myeloid leukemia: focusing on the role of monoclonal antibodies, hypomethylating agents and the leukemic microenvironment. Int. J. Mol. Sci. *18*, e1660.
5. Colovic, M., Colovic, N., Radojkovic, M., Stanisavljevic, D., Kraguljac, N., Jankovic, G., Tomin, D., Suvajdzic, N., Vidovic, A., and Atkinson, H.D. (2012). Induction chemotherapy versus palliative treatment for acute myeloid leukemia in a consecutive cohort of elderly patients. Ann. Hematol. *91*, 1363–1370.
6. Brandwein, J.M., Zhu, N., Kumar, R., Leber, B., Sabloff, M., Sandhu, I., Kassis, J., Olney, H.J., Elemary, M., and Schuh, A.C. (2017). Treatment of older patients with acute myeloid leukemia (AML): revised Canadian consensus guidelines. Am. J. Blood Res. *7*, 30–40.
7. Melzer, M.K., Lopez-Martinez, A., and Altomonte, J. (2017). Oncolytic vesicular stomatitis virus as a viro-immunotherapy: defeating cancer with a "hammer" and "anvil". Biomedicines *5*, e8.
8. Russell, S.J., Peng, K.W., and Bell, J.C. (2012). Oncolytic virotherapy. Nat. Biotechnol. *30*, 658–670.
9. Brunner, K.T., Hurez, D., McCluskey, R.T., and Benacerraf, B. (1960). Blood clearance of P32-labeled vesicular stomatitis and Newcastle disease viruses by the reticuloendothelial system in mice. J. Immunol. *85*, 99–105.
10. Ferguson, M.S., Lemoine, N.R., and Wang, Y. (2012). Systemic delivery of oncolytic viruses: hopes and hurdles. Adv. Virol. *2012*, 805629.
11. Mills, B.J., Beebe, D.P., and Cooper, N.R. (1979). Antibody-independent neutralization of vesicular stomatitis virus by human complement. II. Formation of VSV-lipoprotein complexes in human serum and complement-dependent viral lysis. J. Immunol. *123*, 2518–2524.
12. Harrington, K., Alvarez-Vallina, L., Crittenden, M., Gough, M., Chong, H., Diaz, R.M., Vassaux, G., Lemoine, N., and Vile, R. (2002). Cells as vehicles for cancer gene therapy: the missing link between targeted vectors and systemic delivery? Hum. Gene Ther. *13*, 1263–1280.
13. Willmon, C., Harrington, K., Kottke, T., Prestwich, R., Melcher, A., and Vile, R. (2009). Cell carriers for oncolytic viruses: Fed Ex for cancer therapy. Mol. Ther. *17*, 1667–1676.
14. Roy, D.G., and Bell, J.C. (2013). Cell carriers for oncolytic viruses: current challenges and future directions. Oncolytic Virother. *2*, 47–56.
15. Rommelfanger, D.M., Wongthida, P., Diaz, R.M., Kaluza, K.M., Thompson, J.M., Kottke, T.J., and Vile, R.G. (2012). Systemic combination virotherapy for melanoma with tumor antigen-expressing vesicular stomatitis virus and adoptive T-cell transfer. Cancer Res. *72*, 4753–4764.
16. Wongthida, P., Diaz, R.M., Pulido, C., Rommelfanger, D., Galivo, F., Kaluza, K., Kottke, T., Thompson, J., Melcher, A., and Vile, R. (2011). Activating systemic T-cell immunity against self tumor antigens to support oncolytic virotherapy with vesicular stomatitis virus. Hum. Gene Ther. *22*, 1343–1353.
17. Diaz, R.M., Galivo, F., Kottke, T., Wongthida, P., Qiao, J., Thompson, J., Valdes, M., Barber, G., and Vile, R.G. (2007). Oncolytic immunovirotherapy for melanoma using vesicular stomatitis virus. Cancer Res. *67*, 2840–2848.
18. Qiao, J., Wang, H., Kottke, T., Diaz, R.M., Willmon, C., Hudacek, A., Thompson, J., Parato, K., Bell, J., Naik, J., et al. (2008). Loading of oncolytic vesicular stomatitis virus onto antigen-specific T cells enhances the efficacy of adoptive T-cell therapy of tumors. Gene Ther. *15*, 604–616.
19. Kottke, T., Diaz, R.M., Kaluza, K., Pulido, J., Galivo, F., Wongthida, P., Thompson, J., Willmon, C., Barber, G.N., Chester, J., et al. (2008). Use of biological therapy to enhance both virotherapy and adoptive T-cell therapy for cancer. Mol. Ther. *16*, 1910–1918.
20. VanSeggelen, H., Tantalo, D.G., Afsahi, A., Hammill, J.A., and Bramson, J.L. (2015). Chimeric antigen receptor-engineered T cells as oncolytic virus carriers. Mol. Ther. Oncolytics *2*, 15014.
21. Altomonte, J., Wu, L., Meseck, M., Chen, L., Ebert, O., Garcia-Sastre, A., Fallon, J., Mandeli, J., and Woo, S.L. (2009). Enhanced oncolytic potency of vesicular stomatitis virus through vector-mediated inhibition of NK and NKT cells. Cancer Gene Ther. *16*, 266–278.
22. Muñoz-Álvarez, K.A., Altomonte, J., Laitinen, I., Ziegler, S., Steiger, K., Esposito, I., Schmid, R.M., and Ebert, O. (2015). PET imaging of oncolytic VSV expressing the mutant HSV-1 thymidine kinase transgene in a preclinical HCC rat model. Mol. Ther. *23*, 728–736.
23. Altomonte, J., Braren, R., Schulz, S., Marozin, S., Rummeny, E.J., Schmid, R.M., and Ebert, O. (2008). Synergistic antitumor effects of transarterial viroembolization for multifocal hepatocellular carcinoma in rats. Hepatology *48*, 1864–1873.
24. Altomonte, J., Wu, L., Chen, L., Meseck, M., Ebert, O., García-Sastre, A., Fallon, J., and Woo, S.L. (2008). Exponential enhancement of oncolytic vesicular stomatitis virus potency by vector-mediated suppression of inflammatory responses in vivo. Mol. Ther. *16*, 146–153.
25. Marozin, S., Altomonte, J., Muñoz-Álvarez, K.A., Rizzani, A., De Toni, E.N., Thasler, W.E., Schmid, R.M., and Ebert, O. (2015). STAT3 inhibition reduces toxicity of oncolytic VSV and provides a potentially synergistic combination therapy for hepatocellular carcinoma. Cancer Gene Ther. *22*, 317–325.
26. Johnson, J.E., Nasar, F., Coleman, J.W., Price, R.E., Javadian, A., Draper, K., Lee, M., Reilly, P.A., Clarke, D.K., Hendry, R.M., and Udem, S.A. (2007). Neurovirulence properties of recombinant vesicular stomatitis virus vectors in non-human primates. Virology *360*, 36–49.
27. van den Pol, A.N., Dalton, K.P., and Rose, J.K. (2002). Relative neurotropism of a recombinant rhabdovirus expressing a green fluorescent envelope glycoprotein. J. Virol. *76*, 1309–1327.
28. Felt, S.A., and Grdzelishvili, V.Z. (2017). Recent advances in vesicular stomatitis virus-based oncolytic virotherapy: a 5-year update. J. Gen. Virol. *98*, 2895–2911.
29. Klar, R., Schober, S., Rami, M., Mall, S., Merl, J., Hauck, S.M., Ueffing, M., Admon, A., Slotta-Huspenina, J., Schwaiger, M., et al. (2014). Therapeutic targeting of naturally presented myeloperoxidase-derived HLA peptide ligands on myeloid leukemia cells by TCR-transgenic T cells. Leukemia *28*, 2355–2366.
30. Mall, S., Yusufi, N., Wagner, R., Klar, R., Bianchi, H., Steiger, K., Straub, M., Audehm, S., Laitinen, I., Aichler, M., et al. (2016). Immuno-PET imaging of engineered human T cells in tumors. Cancer Res. *76*, 4113–4123.
31. Yusufi, N., Mall, S., Bianchi, H.O., Steiger, K., Reder, S., Klar, R., Audehm, S., Mustafa, M., Nekolla, S., Peschel, C., et al. (2017). In-depth characterization of a TCR-specific tracer for sensitive detection of tumor-directed transgenic T cells by immuno-PET. Theranostics *7*, 2402–2416.
32. Sommermeyer, D., Hudecek, M., Kosasih, P.L., Gogishvili, T., Maloney, D.G., Turtle, C.J., and Riddell, S.R. (2016). Chimeric antigen receptor-modified T cells derived from defined CD8+ and CD4+ subsets confer superior antitumor reactivity in vivo. Leukemia *30*, 492–500.
33. Wang, X., Berger, C., Wong, C.W., Forman, S.J., Riddell, S.R., and Jensen, M.C. (2011). Engraftment of human central memory-derived effector CD8+ T cells in immunodeficient mice. Blood *117*, 1888–1898.
34. Oliere, S., Arguello, M., Mesplede, T., Tumilasci, V., Nakhaei, P., Stojdl, D., Sonenberg, N., Bell, J., and Hiscott, J. (2008). Vesicular stomatitis virus oncolysis of

T lymphocytes requires cell cycle entry and translation initiation. J. Virol. *82*, 5735–5749.

35. Tan, H., Derrick, J., Hong, J., Sanda, C., Grosse, W.M., Edenberg, H.J., Taylor, M., Seiwert, S., and Blatt, L.M. (2005). Global transcriptional profiling demonstrates the combination of type I and type II interferon enhances antiviral and immune responses at clinically relevant doses. J. Interferon Cytokine Res. *25*, 632–649.
36. Kaluza, K.M., Thompson, J.M., Kottke, T.J., Flynn Gilmer, H.C., Knutson, D.L., and Vile, R.G. (2012). Adoptive T cell therapy promotes the emergence of genomically altered tumor escape variants. Int. J. Cancer *131*, 844–854.
37. Bai, X.F., Liu, J., Li, O., Zheng, P., and Liu, Y. (2003). Antigenic drift as a mechanism for tumor evasion of destruction by cytolytic T lymphocytes. J. Clin. Invest. *111*, 1487–1496.
38. Bai, X.F., Liu, J.Q., Joshi, P.S., Wang, L., Yin, L., Labanowska, J., Heerema, N., Zheng, P., and Liu, Y. (2006). Different lineages of P1A-expressing cancer cells use divergent modes of immune evasion for T-cell adoptive therapy. Cancer Res. *66*, 8241–8249.
39. Shultz, L.D., Schweitzer, P.A., Christianson, S.W., Gott, B., Schweitzer, I.B., Tennent, B., McKenna, S., Mobraaten, L., Rajan, T.V., Greiner, D.L., et al. (1995). Multiple defects in innate and adaptive immunologic function in NOD/LtSz-scid mice. J. Immunol. *154*, 180–191.
40. Ravichandran, K.S. (2010). Find-me and eat-me signals in apoptotic cell clearance: progress and conundrums. J. Exp. Med. *207*, 1807–1817.
41. Poon, I.K., Lucas, C.D., Rossi, A.G., and Ravichandran, K.S. (2014). Apoptotic cell clearance: basic biology and therapeutic potential. Nat. Rev. Immunol. *14*, 166–180.
42. Abdullahi, S., Jakel, M., Behrend, S.J., Steiger, K., Topping, G., Krabbe, T., Colombo, A., Sandig, V., Schiergens, T.S., Thasler, W.E., et al. (2018). A novel chimeric oncolytic virus vector for improved safety and efficacy as a platform for the treatment of hepatocellular carcinoma. J. Virol. *92*, e01386–18.
43. Muik, A., Kneiske, I., Werbizki, M., Wilflingseder, D., Giroglou, T., Ebert, O., Kraft, A., Dietrich, U., Zimmer, G., Momma, S., and von Laer, D. (2011). Pseudotyping vesicular stomatitis virus with lymphocytic choriomeningitis virus glycoproteins enhances infectivity for glioma cells and minimizes neurotropism. J. Virol. *85*, 5679–5684.
44. Zhang, L., Steele, M.B., Jenks, N., Grell, J., Suksanpaisan, L., Naik, S., Federspiel, M.J., Lacy, M.Q., Russell, S.J., and Peng, K.W. (2016). Safety studies in tumor and non-tumor-bearing mice in support of clinical trials using oncolytic VSV-IFNβ-NIS. Hum. Gene Ther. Clin. Dev. *27*, 111–122.
45. Covassin, L., Jangalwe, S., Jouvet, N., Laning, J., Burzenski, L., Shultz, L.D., and Brehm, M.A. (2013). Human immune system development and survival of non-obese diabetic (NOD)-scid IL2rγ(null) (NSG) mice engrafted with human thymus and autologous haematopoietic stem cells. Clin. Exp. Immunol. *174*, 372–388.
46. Ebert, O., Shinozaki, K., Huang, T.G., Savontaus, M.J., García-Sastre, A., and Woo, S.L. (2003). Oncolytic vesicular stomatitis virus for treatment of orthotopic hepatocellular carcinoma in immune-competent rats. Cancer Res. *63*, 3605–3611.
47. Le Tourneau, C., Lee, J.J., and Siu, L.L. (2009). Dose escalation methods in phase I cancer clinical trials. J. Natl. Cancer Inst. *101*, 708–720.

OMTO, Volume *12*

Supplemental Information

Enhanced Safety and Efficacy of Oncolytic VSV Therapy by Combination with T Cell Receptor Transgenic T Cells as Carriers

Michael Karl Melzer, Lisa Zeitlinger, Sabine Mall, Katja Steiger, Roland M. Schmid, Oliver Ebert, Angela Krackhardt, and Jennifer Altomonte

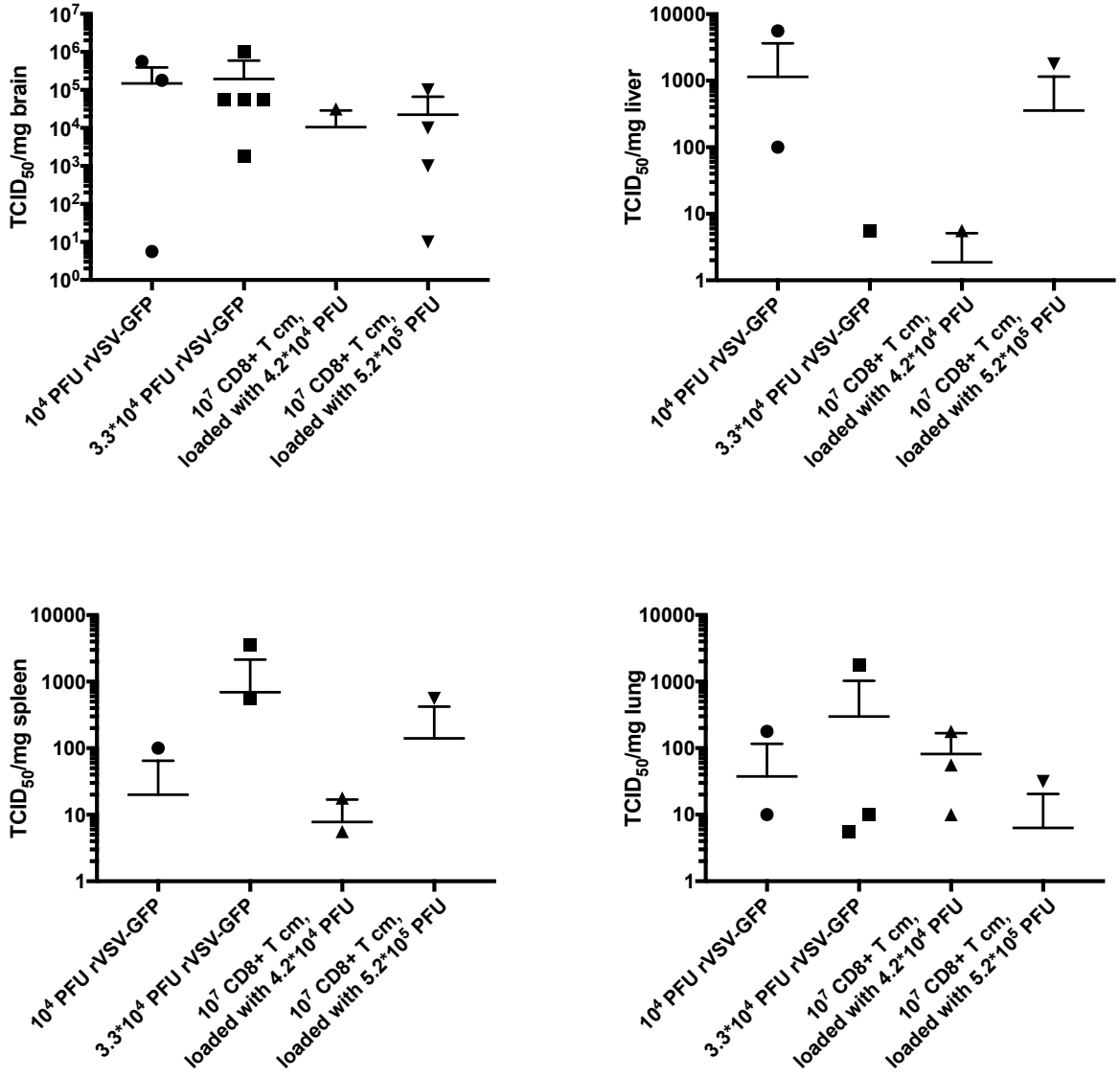

Supplementary Figure 1. VSV demonstrates off-target replication in NSG mice.

TCID50 assays were performed to quantify replication competent rVSV-GFP in the major organs of NSG mice following systemic treatment. Titers recovered from brain (A), liver (B), spleen (C) and lungs (D) are shown (N=3-6). Individual data points and means ± standard deviation are plotted. Replication competent virus was also found in some mice in the heart, kidney, intestine and pancreas (data not shown).

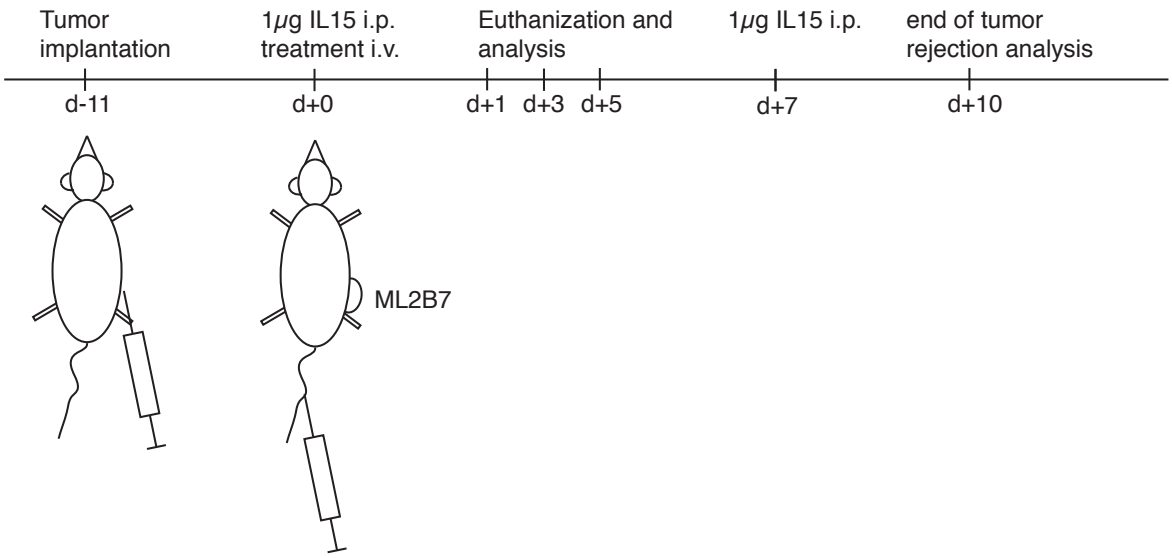

Supplementary Figure 2. Treatment model.

10^7 ML2B7 tumor cells were implanted subcutaneously into the right flank of NSG mice. After 11 days (for kinetic experiments) mice were tail vein injected with different therapies: 1. 10^7 TCR CD8+ T cm; 2. 10^7 control CD8+ T cm; 3. 10^7 TCR CD8+ T cm infected with rVSV-tk at MOI 0.1; 4. 10^7 control CD8+ T cm infected with rVSV-tk at MOI 0.1; 5. 10^4 PFU rVSV-tk, 6. PBS. On day 1,3 and 5 post injection mice were sacrificed and tumors were analyzed by FACS, TCID50 and histology. Tumor rejection was followed for 10 days after treatment. Survival was followed until ML2B7 tumors reached 2cm or mice showed severe signs of sickness, weight loss of more than 20% or were impaired in their ability to walk.

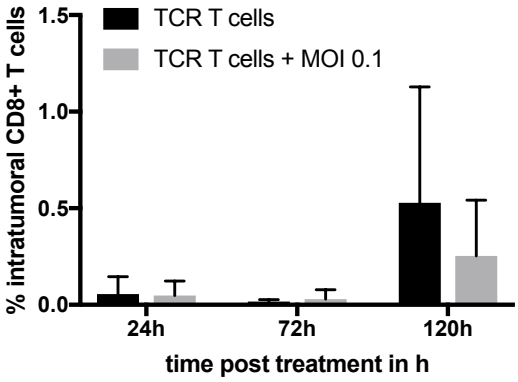

Supplementary Figure 3: Specific proliferation of TCR T cells in their target tumor.

Tumor bearing NSG mice were treated systemically with the indicated TCR cells, with or without rVSV-tk, and euthanized after 24h, 72h and 120h. The percentages of intratumoral CD8+ T cells were determined by FACS analysis. Mean and SD are given. N=3-5.

Listing of detailed numbers of used mice per group

Group	10^4 PFU VSV-GFP	$3.3*10^4$ PFU VSV-GFP	10^7 CD8+ T cm, MOI 0.1	10^7 CD8+ T cm, MOI 1
Figure 4A	6	6	3	6
Figure 4B	5	6	3	5

Supplementary table 1: Number of mice for figure 4

Group	TCR T cells	Control T cells	TCR T cells +VSV	Control T cells + VSV	VSV	PBS
Figure 5A	5	3	5	5	5	3
Figure 5B			6	6	4	

Supplementary table 2: Number of mice for figure 5

Group	TCR T cells	Control T cells	TCR T cells +VSV	Control T cells + VSV	VSV	PBS
Figure 6A	5	3	5	5	5	3
Figure 6B	5	3	5	5	5	3
Figure 6D	6	5	5	4	6	5

Supplementary table 3: Number of mice for figure 6

Group	10^4 PFU VSV-GFP	$3.3*10^4$ PFU VSV-GFP	10^7 CD8+ T cm, MOI 0.1	10^7 CD8+ T cm, MOI 1
Sup. Fig. 1A	5	6	3	5
Sup. Fig. 1B	5	6	3	5
Sup. Fig. 1C	5	6	3	4
Sup. Fig. 1D	5	6	3	5

Supplementary table 4: Number of mice for supplementary figure 1

Group	TCR T cells	TCR T cells + MOI 0.1 rVSV-tk
24h after therapy	3	4
72h after therapy	5	3
120h after therapy	5	5

Supplementary table 5: Number of mice for supplementary figure 3